

RESEARCH

Open Access



Effects of simulated atmospheric nitrogen deposition on the bacterial community structure and diversity of four distinct biocolonization types on stone monuments: a case study of the Leshan Giant Buddha, a world heritage site

Xuli Chen¹, Huixing Song^{2*}, Bo Sun³ and Tianyu Yang⁴

Abstract

Atmospheric nitrogen deposition may affect the biodeterioration process of stone monuments through direct and indirect pathways, but relevant studies are lacking. Therefore, taking the biologically colonized rocks around the Leshan Giant Buddha (World Heritage - Mixed Property) as the research objects, we studied the effects of multiple nitrogen addition levels (0, 9, 18, 36, 72 kg N hm⁻² a⁻¹; N0, N1; N2; N3; N4) on the bacterial community structure and soil nutrients on the surfaces of stones with four biocolonization types, including naked rock (NR), and lichen (LR), bryophyte (BS) and vascular plant (VS) colonization, to investigate the potential effect of atmospheric nitrogen deposition on the rock weathering of the Leshan Giant Buddha. The results demonstrated that nitrogen addition impacted soil carbon, nitrogen and phosphorus nutrients, as well as bacterial community structure and composition, but the responses to nitrogen input varied among different colonization types. Nitrogen fertilization promoted the accumulation of total organic carbon and total nitrogen in NR and LR, and increased the content of total phosphorus in VS. Bacterial α -diversity decreased with nitrogen addition in NR but increased with nitrogen addition in VS. Nitrogen addition significantly ($R > 0.9$, $p < 0.01$) changed the bacterial community composition in the four biocolonization types, and the changes were dominated by species replacement (contributed to 60.98%, 76.32%, 67.27% and 72.14% for bacterial diversity in NR, LR, BS and VS, respectively). Total nitrogen, dissolved organic nitrogen, dissolved organic nitrogen and total phosphorus were the most important ecological factors affecting bacterial community structure in NR, LR, BS and VS, respectively. Nitrogen addition enriched different bacterial taxa in the four biocolonization types. The results of this study provide basic data for the protection of stone monuments and the formulation of sustainable development strategies under a changing climate.

Keywords Stone monuments, Biocolonization, Biodeterioration, Nitrogen deposition, Bacterial diversity, Community composition, Leshan Giant Buddha

*Correspondence:

Huixing Song
Songhuixing@sicau.edu.cn

Full list of author information is available at the end of the article



© The Author(s) 2024. **Open Access** This article is licensed under a Creative Commons Attribution 4.0 International License, which permits use, sharing, adaptation, distribution and reproduction in any medium or format, as long as you give appropriate credit to the original author(s) and the source, provide a link to the Creative Commons licence, and indicate if changes were made. The images or other third party material in this article are included in the article's Creative Commons licence, unless indicated otherwise in a credit line to the material. If material is not included in the article's Creative Commons licence and your intended use is not permitted by statutory regulation or exceeds the permitted use, you will need to obtain permission directly from the copyright holder. To view a copy of this licence, visit <http://creativecommons.org/licenses/by/4.0/>. The Creative Commons Public Domain Dedication waiver (<http://creativecommons.org/publicdomain/zero/1.0/>) applies to the data made available in this article, unless otherwise stated in a credit line to the data.

Introduction

Stone monuments are nonrenewable relics with historical, artistic, cultural, scientific and technological value produced by human historical activities that are made of stone and are vectors of historical information and witnesses of human civilization [1]. Stone can provide living organisms with abundant mineral elements such as calcium, iron, magnesium, aluminium, and sodium. Therefore, immovable stone artefacts that are directly exposed to the atmosphere (in natural and artificial environments) often serve as substrates for colonization by various organisms [1]. To survive and reproduce, these organisms carry out a series of life activities (including biophysical and biochemical processes) on the stone substrate that can cause irreversible damage to the cultural relic, which is called biodeterioration. The biogeochemical cycle, a natural cyclic process that converts stones into sand and soil, is believed to be the fundamental mechanism underlying biodegradation, which plays a crucial role in sustaining life on Earth [2]. However, biodeterioration occurring on stone artefacts will lead to a permanent loss of cultural heritage.

Microorganisms play an important role in biodeterioration in any natural rocky ecosystem, as they are the organisms responsible for the transformation, recycling and degradation of various nutrient substances [3]. In the initial stage of biodegradation, a diverse array of microorganisms forms a biofilm matrix on the surface of exposed rock, thereby initiating the degradation process through vital activities such as cellular proliferation, secretion of corrosive acids, and REDOX reactions [4]. Lithophytic lichens employ a cooperative strategy to facilitate the erosion of rock substrates, whereby photosynthetic commensal microorganisms generate energy through photosynthesis, followed by chemical erosion facilitated by the secretion of lichenic acid and polyphenols from mycobionts [5]. In addition, it has been reported that root exudates of higher plants, such as carbohydrates, amino acids and proteins, as well as plant residues and litter, which increase moisture and organic matter content on stone surfaces, are beneficial to the microorganism growth of the local rhizosphere and promote the biodeterioration efficiency of stone [6]. Thus, microorganisms in stone habitats not only directly promote the biophysical and biochemical degradation processes of stone matrix, but also interact with other organisms to promote mineral decomposition, indirectly [2, 7]. Direct evidence has shown that photosynthetic bacteria use light energy to assimilate inorganic carbon (CO₂) into organic carbon, which is deposited and enriched on the stone surface, creating nutrient conditions for the formation of microbial communities, including aerobic and anaerobic microorganisms [8]. Bacteria can also

take pyrite, biotite and amphibole rich in reduced iron as food, obtain energy through the oxidation–reduction process of ferrous ions, and accelerate the weathering and decomposition of stone [9]. Stone biodegradation is rarely associated with one or a few microbial species. Microbial communities usually establish complex interspecific interactions in barren stone substrates to enhance biodegradation efficiency by synergistic interactions [10, 11]. In view of this, it is vital to understand the structure and diversity of bacterial communities in various habitats on stone to understand the potential risks of biodeterioration on stone monuments.

Over the past century, reactive nitrogen (Nr) content produced by human activities such as agricultural production, fossil fuel combustion and industrial emissions has increased approximately 10-fold [12], exceeding natural N fixation [13], directly expanding the atmospheric Nr content and increasing the atmospheric Nr deposition rate [14]. Based on the current anthropogenic atmospheric Nr emissions, global atmospheric N deposition is expected to double by 2050 compared to 1995 [15]. With rapid economic development, China has become the third major N deposition region after Europe and the United States [16–18]. From 1980 to 2020, atmospheric N deposition in China showed an upwards trend [18]. Many studies have found that increased atmospheric N deposition significantly affects soil microbial community composition, diversity and activity [19–21]. Additionally, the deposition of pollutants from the atmosphere on the stone surface can affect microbial colonization and degradation and may accelerate biodeterioration [2]. At present, we found no studies with atmospheric Nr deposition on microorganisms in stone monuments with different biodeterioration. Analysing the responses of microbial communities of different biocolonization types on stone monuments to Nr deposition is essential to predict the biodeterioration of stone monuments under scenarios of increased anthropogenic Nr deposition.

The Leshan Giant Buddha is the largest ancient stone statue of the Maitreya Buddha in the world [22]. It was initially undertaken during the early Kaiyuan period of the Tang Dynasty (AD 713) and required a span of 90 years for its completion. It epitomizes the pinnacle of stone carving art during the Tang Dynasty, boasting immense historical, artistic, and scientific significance. In December 1996, it was designated as a “World Cultural and Natural Heritage” site by UNESCO in conjunction with the Mount Emei Nature Reserve. After more than a thousand years of sun and rain, combined with the influence of tourists and modern environmental pollution, the Leshan Giant Buddha body and its surrounding sandstone mountains not only have attached algae-bacterial symbionts but are also colonized by various organisms,

including lichens, bryophytes and vascular plants. Previous studies have shown that the bacterial communities in different biocolonization areas of the Leshan Giant Buddha body are significantly different [23]. Nitrogen-containing compounds released by human activities interact with water vapour in the atmosphere and deposit on the surface of outdoor stone artefacts [24], becoming a source of nutrients for epilithic microbes, thereby indirectly affecting the biodeterioration process of cultural relics. Although many existing studies have reported the community composition of epilithic microorganisms on stone monuments, we lack a predictive understanding of how microbial communities respond to nutrient inputs from different environmental gradients. Therefore, a mountain around the Leshan Giant Buddha body with the same lithology as the giant Buddha was selected as the sample site, and a N deposition simulation experiment was conducted to study the responses of bacterial communities and soil physical and chemical properties to N addition under different biocolonization types to assess the effects of atmospheric N deposition on the biodeterioration of the Leshan Giant Buddha. Our results contribute to understanding the ecological mechanism of biodeterioration of stone monuments under changing environments and provide basic data for

sustainable conservation strategies of outdoor immovable stone artefacts.

Materials and methods

Experimental site and sample collection

The Leshan Giant Buddha scenic area is located in Leshan City, Sichuan Province, China (latitude 29°32' 47" N, longitude 103°45' 48" E) (Fig. 1). The Leshan Giant Buddha body is chiselled on the red sandstone of Qiluan Peak on Lingyun Mountain at the junction of the Dadu River and Min River. The study area has a typical subtropical humid monsoon climate, with abundant precipitation, of which the average annual precipitation is approximately 1291.6 mm and is mainly concentrated in summer, accounting for 58% of the annual precipitation. The average annual evaporation is 1057 mm, and the relative humidity is as high as 81%. The vegetation type around the giant Buddha is subtropical evergreen broadleaved forest, dominated by *Castanopsis* spp., *Cyclobalanopsis* spp., and *Schima superba*.

The experiment was conducted in a red sandstone hill around the Leshan Giant Buddha, which is colonized by the same organism types (such as lichens, bryophytes and vascular plants) as the Buddha's body. Four stone biocolonization, including naked rock (NR), lichen (LR),

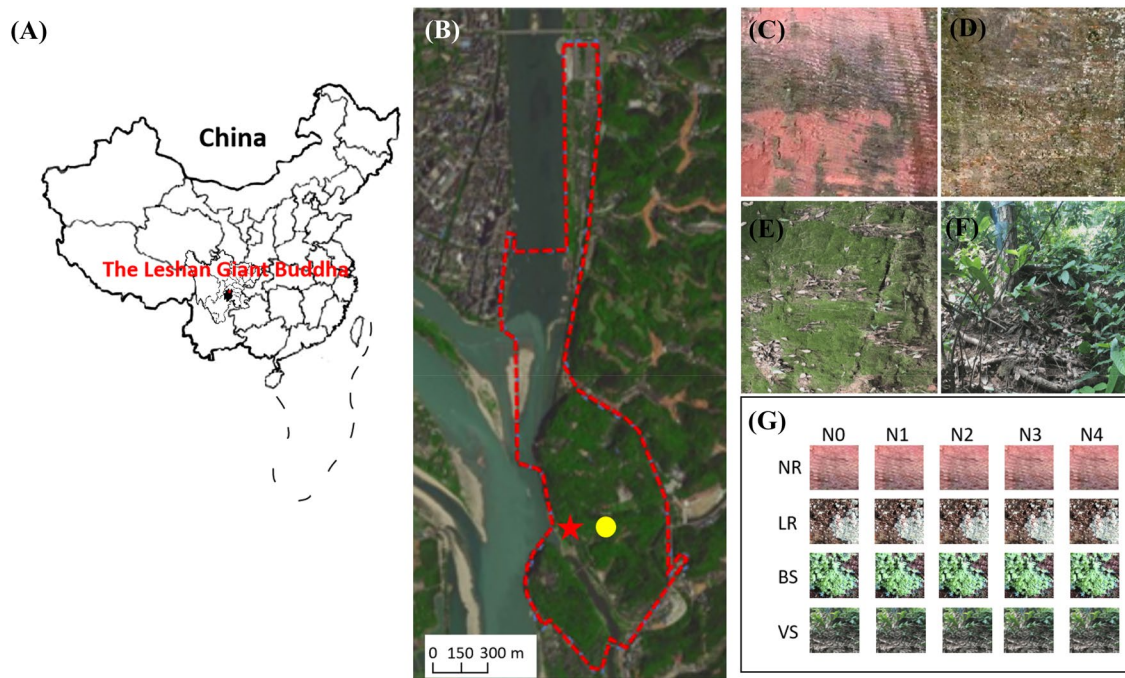


Fig. 1 Location of the Leshan Giant Buddha and test site. **A** Location of the Leshan Giant Buddha; **B** position of the giant Buddha body and experimental test plot; **C** naked rock (NR) sample site; **D** lichen-colonized (LR) sample site; **E** bryophyte-colonized (BS) sample site; **F** vascular-colonized (VS) sample site. **G**, schematic diagram of plot layout

bryophyte (BS) and vascular plant (VS) cover, which had the same weathering status as the giant Buddha body, were selected as the treatment objects for the N deposition simulation experiment. According to the local N deposition situation of the Sichuan Basin, which was 36 kg N ha⁻¹ yr⁻¹ and dominated by ammonium and nitrate nitrogen [25], we took twice the actual annual N wet deposition as the maximum predicted value, set the N addition amount in a way that decreased exponentially, and set five N rates (0, 9, 18, 36, and 72 kg N ha⁻¹ yr⁻¹; N0, N1, N2, N3, and N4, respectively) with NH₄NO₃ as the N source. Three duplicate quadrats were set for each N rate, for a total of 60 treated quadrats, each of which had dimensions of 2 × 2 m².

The concentration and amount of ammonium nitrate solution that needed to be sprayed in each sample plot were calculated according to the distribution of annual precipitation and monthly precipitation in the region. Since October 2018, a hand-held electric sprayer has been used to spray each test site in sunny weather in the first ten days of each month. To avoid interaction between the plots, a buffer zone of more than 1.0 m was reserved between the plots. The treatment continued for 24 months. Approximately 30 g of rock debris/soil was collected according to multi-point sampling method using a sterile knife, thoroughly mixed, and securely packed in an aseptic plastic sealing bag. One sample was obtained from each treatment quadrat, resulting in a total of 60 samples that were promptly placed in a sampling box with an ice pack and transported to the laboratory on the same day. Each sample was evenly divided into two portions: one portion was naturally dried for chemical property analysis, while the other portion underwent removal of animal and plant residues, gravel, and other impurities at 4°C. For larger samples, they were mashed, sieved through a 2 mm mesh screen, appropriately labeled, and stored at -80°C in the refrigerator for subsequent sequencing analysis.

Physicochemical property determination of soil samples

The pH of the soil samples was determined by the potentiometric method (soil to water ratio 2.5:1) after drying, grinding, cleaning and sifting (PHS-3 C, LEICI, Shanghai, China). The content of total organic carbon (TOC) was determined by K₂Cr₂O₇-H₂SO₄ oxidation and FeSO₄ titration [26]. The total nitrogen (TN) content was determined by concentrated sulfuric acid and the Kjeldahl method (KND, Top Ltd., Hangzhou, Zhejiang, China). The total phosphorus (TP) content was determined by perchloric acid-sulfuric acid oxidation and the molybdenum antimony resistance colorimetric method [27]. The contents of dissolved organic carbon (DOC) and dissolved organic nitrogen (DON) in the soil solution

filtered by the 0.45 μm filter membrane were measured by an organic carbon analyser (TOC-CPH, Shimadzu Corporation). The ammonium nitrogen (NH₄⁺-N) and nitrate nitrogen (NO₃⁻-N) contents of the soil samples were extracted using 2 mol·L⁻¹ KCl solution at a ratio of 1:5 and measured by a spectrophotometric method [28].

Extraction and PCR amplification of the 16 S rRNA gene

Total DNA extraction was performed according to the E.Z.N.A.[®] soil DNA kit (Omega Biotek, Norcross, GA, U.S.), and the quality of DNA extraction was measured using 1% AGAR gel electrophoresis. DNA concentration and purity were determined using a NanoDrop2000. The primers 338F (5'-ACTCCTACGGGAGGCAGCAG-3') and 806R (5'-GGACTACHVGGGTWTCTAAT-3') were used to amplify the V3-V4 variable region of the 16 S rRNA gene [29, 30].

Illumina MiSeq sequencing and bioinformatics analysis

The raw data were filtered by quality control and sequence correction to obtain optimized sequences. A total of 2907454 optimized sequences were obtained from 60 samples. In the NR, LR, BS and VS habitats, a total of 740394, 756210, 693191 and 717659 sequences were obtained, respectively; an average of 49306, 50414, 46213, and 47844 sequences were obtained for each sample, respectively. Each operational taxonomic unit (OTU) was deduplicated, clustered and chimera detected by UPARSE [31, 32] software (<http://drive5.com/uparse/>, version 7.1), and the nonrepetitive sequences were clustered according to 97% similarity to obtain the representative sequences of OTUs. Each sequence was annotated for species classification using RDP Classifier [33] (<http://rdp.cme.msu.edu/>, version 2.2) and aligned against the Silva 16 S rRNA database, with an alignment confidence threshold of 70%. The α-diversity was utilized to evaluate the richness and diversity of bacterial communities, which were quantified by the Chao1 index for community richness and the Shannon index for community diversity. All these sequences from this study were deposited in Genbank with accession number SRP451507.

Data statistical analysis

SPSS (Version 20.0, IBM, New York, NY, USA) was used to compare the significance of each index among different N application treatments using one-way analysis of variance (ANOVA) and Student's t test ($p < 0.05$). QIIME software was used to generate abundance tables at each taxonomic level. Mothur (Version 1.30.2) was used to calculate the Chao1 and Shannon indices of bacterial α-diversity. The Bray-Curtis distance matrix and QIIME software were used to calculate the β-diversity distance of bacteria. Principal coordinate analysis (PCoA) was

performed using the ape package of R (Version 3.3.1). Analysis of similarities (ANOSIM) was used to test the differences in bacterial communities among different groups, and permutational multivariate analysis of variance (PERMANOVA) was used to analyze the explanation of sample variance by different grouping factors. Compositional dissimilarities among sites (beta diversity) were partitioned into replacement and richness difference components (Podani family, Sørensen dissimilarities) using the R package *adespatial* [34]. The *ggplots2* package was then used for visualization of PCoA and trioriginal plots. Multivariate linear discrimination and effect size analysis (LEfSe) and graphical visualization were performed by LEfSe software [35].

Results

Soil physicochemical properties

According to the results, N addition significantly increased TOC content in NR, and only the N1 treatment significantly increased TOC in LR. In contrast, N addition had no significant effect on TOC content in BS and

VS (Fig. 2A). The TN content increased with increasing N addition in NR and increased first and then decreased with increasing N addition in LR, BS and VS (Fig. 2B). The response of soil TP content to N addition was different in the four colonization types. In NR and LR, the TP content decreased after N addition, especially under the N3 and N4 treatments. In BS, the TP content decreased only under the N2 treatment, and there were no significant differences among the other treatments. However, the TP content showed a significant linear increase with increasing N addition in VS (Fig. 2C). The soil DOC content increased after N addition in the four biocolonization types but did not respond consistently to different N addition levels in each disease. In particular, in NR, the DOC content was significantly lower under N2–N4 than under control N0 (Fig. 2D). The DON content significantly increased with N addition in NR, LR, and BS, but it significantly decreased under the N3 and N4 treatments in VS (Fig. 2E). The soil AP content showed a convex curve with N addition in the four biocolonization types, but no significant differences were found in

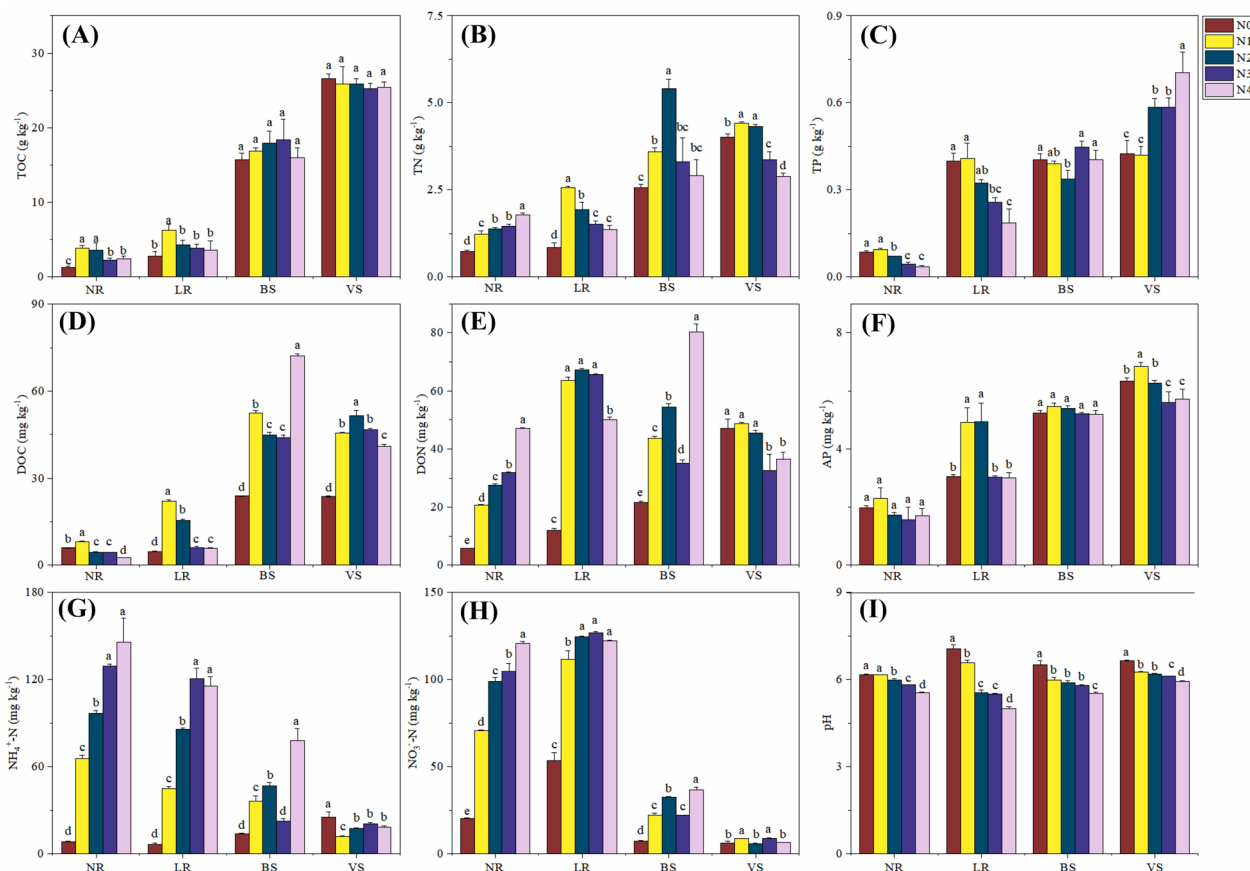


Fig. 2 Soil physicochemical properties of four biocolonization types under multiple nitrogen addition. **A** total organic carbon (TOC); **B** total nitrogen (TN); **C** total phosphorus (TP); **D** dissolved organic carbon (DOC); **E**, dissolved organic nitrogen (DON); **F** available phosphorus (AP); **G** ammonium nitrogen ($\text{NH}_4^+\text{-N}$); **H** nitrate nitrogen ($\text{NO}_3^-\text{-N}$); **I** pH. Values with same letter are not significantly different ($p < 0.05$)

NR and BS (Fig. 2F). In addition, the contents of $\text{NH}_4^+\text{-N}$ and $\text{NO}_3^-\text{-N}$ had the same overall change trend, both of which increased significantly after N addition in NR, LR and BS and showed an S-shaped curve trend in VS. The difference was that N addition significantly decreased the $\text{NH}_4^+\text{-N}$ content in VS (Fig. 2G and H). Obviously, pH decreased linearly with N addition in all four colonization types (Fig. 2I). According to the above results, the responses of carbon, nitrogen and phosphorus nutrients to N addition were different in various habitats, but the pH value showed a consistent downwards trend.

Diversity and composition of bacterial communities

The results of α -diversity analysis showed that N addition significantly reduced bacterial Shannon and Chao1 metrics in NR compared with N0, except for the N3 treatment for Chao1. This suggested that N addition suppressed bacterial community diversity in NR. In LR and BS, the Shannon and Chao1 metrics of the bacterial communities both displayed a hump-shaped pattern with N addition. However, the diversity of bacterial communities showed a contrasting pattern in VS after N addition, with increasing patterns for Shannon and Chao1 metrics (Fig. 3A and B). These results indicated that N addition promoted the richness and diversity of bacterial communities in VS.

PCoA and ANOSIM nonparametric tests were used to evaluate the β -diversity of bacterial communities with N addition in each colonization type, and multivariate analysis of variance (Adonis) was used to evaluate the explanation of the differences between groups. The selected principal axes (PC1 and PC2 axes) explained 69.99%, 80.58%, 62.74% and 72.31% of the

variation in the bacterial community in NR, LR, BS and VS, respectively (Fig. 4A). ANOSIM analysis showed that N addition significantly affected the bacterial community composition in the four biocolonization types (NR: $R=0.9215$, $p=0.001$; LR: $R=0.9215$, $p=0.001$; BS: $R=0.9437$, $p=0.001$; VS: $R=0.9733$, $p=0.001$), and the differences between groups were greater than those within groups (Fig. 4B). Moreover, the results of PERMANOVA analysis showed that N addition explained 82.73% ($p=0.001$), 91.10% ($p=0.001$), 76.15% ($p=0.001$) and 83.36% ($p=0.001$) of the bacterial community discrepancy in NR, LR, BS and VS, respectively (Additional file 1: Table S1). The results indicated that the composition of bacterial communities in the four biocolonization types changed significantly with N addition, which could explain the community variation to a large extent.

The variation in species composition among sites, or beta diversity, can be decomposed into replacement and richness differences, allowing testing of various hypotheses about the processes driving species distribution and biodiversity. The beta diversity decomposition analyses showed that the compositional dissimilarities of the bacterial community were all dominated by species replacement processes in the four biocolonization types (contributed to 60.98%, 76.32%, 67.27% and 72.14% of the bacterial diversity in NR, LR, BS and VS, respectively), while richness difference processes only contributed 39.02%, 23.68%, 32.73% and 27.86% on average (Fig. 5). This indicated that the changes in bacterial diversity caused by N addition in the four biocolonization types were more determined by species turnover than differences in richness.

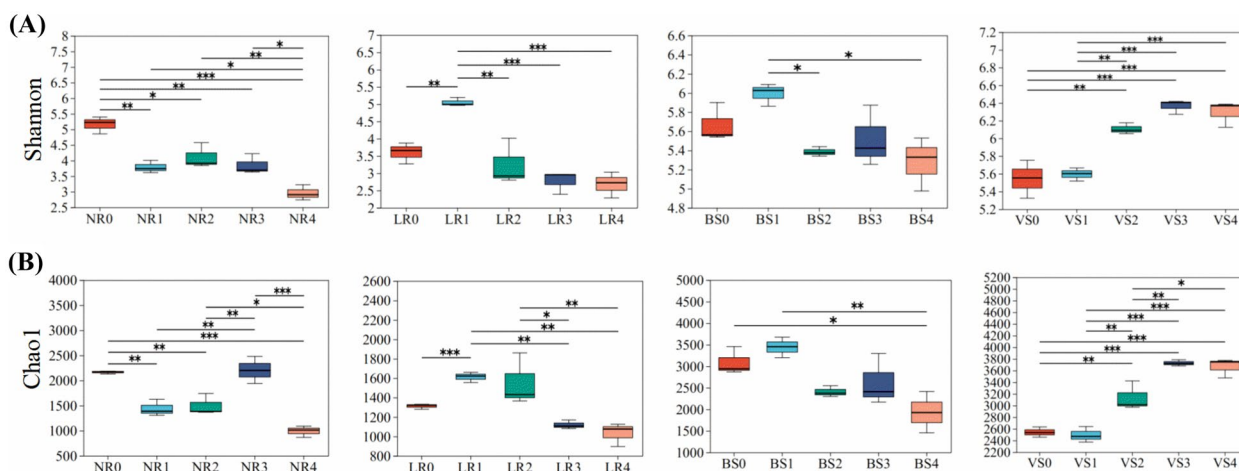


Fig. 3 Shannon (A) and Chao1 (B) indices of bacterial community under different nitrogen addition levels according to one-way ANOVA with Student's t-tests ($p < 0.05$). * indicate significant differences between different treatments. *, $p < 0.05$; **, $p < 0.01$; ***, $p < 0.001$

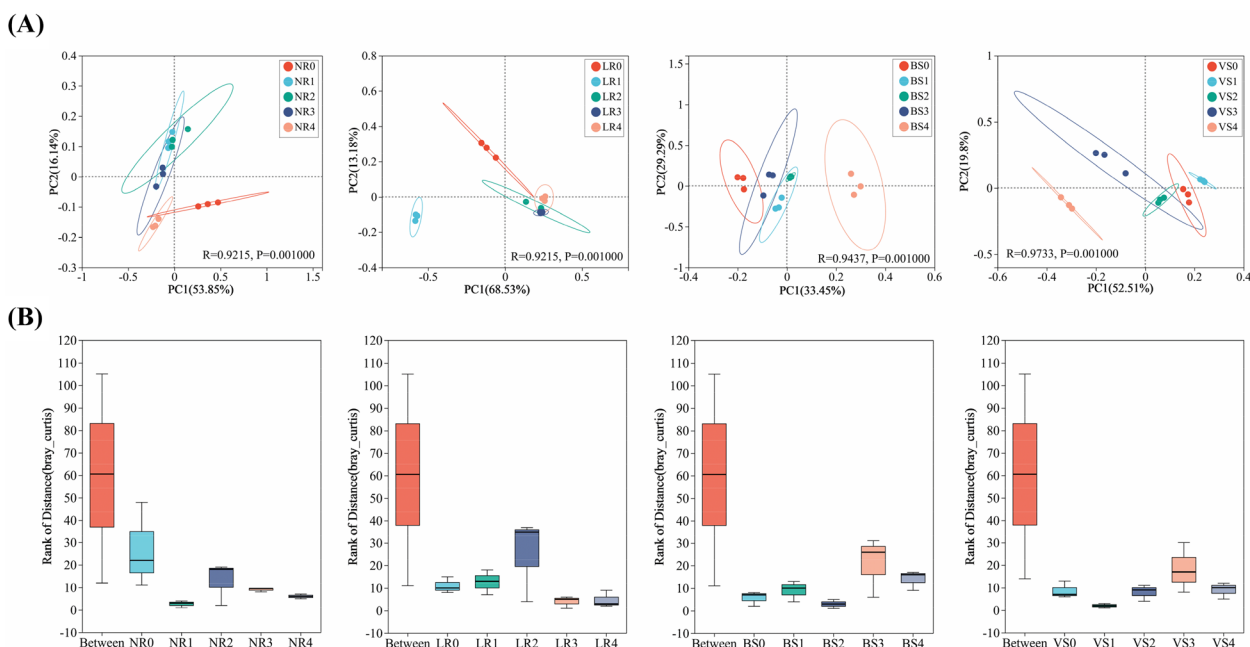
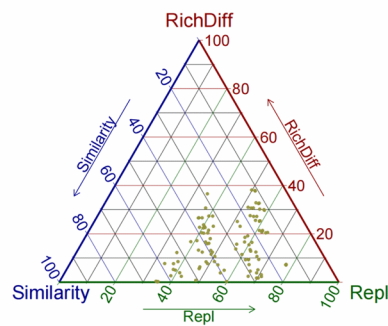
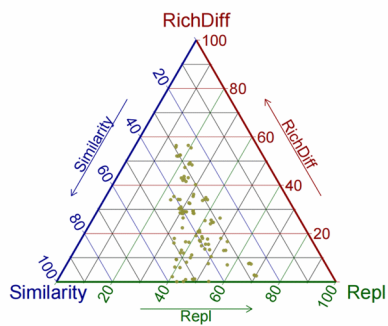


Fig. 4 Analysis of differences in bacterial community structure under different treatments. Principal co-ordinate analysis (PCoA) based on the bray_curtis distance matrix (A). ANOSIM analysis based on bray_curtis distance matrix (B)

(A) $S=0.6909, Repl=0.1885, RichDiff=0.1206$ (n=210 pairs of sites) (B) $S=0.6583, Repl=0.2608, RichDiff=0.0809$ (n=210 pairs of sites)



(C) $S=0.7015, Repl=0.2008, RichDiff=0.0977$ (n=210 pairs of sites) (D) $S=0.7136, Repl=0.2066, RichDiff=0.0798$ (n=210 pairs of sites)

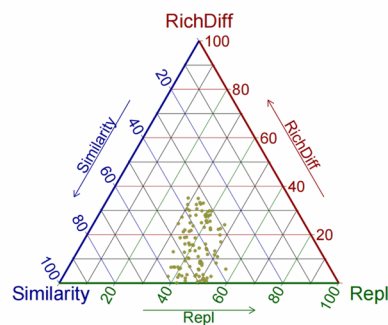
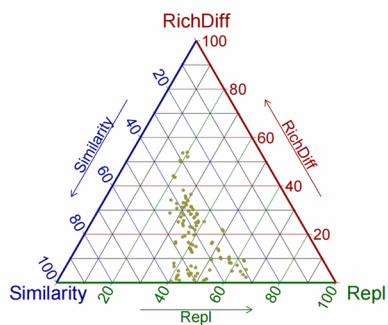


Fig. 5 Triangular plots of beta diversity comparisons (using Sørensen dissimilarity index) for bacteria communities in NR (A), LR (B), BS (C) and VS (D) colonization

Bacterial community composition and relative abundance

Bacterial groups with relative abundances greater than 1% at the phylum taxonomic level were selected and are shown in the histogram of Fig. 6, and the groups with relative abundances less than 1% were combined into others. The dominant bacterial phyla shared by the four biocolonization types included Cyanobacteria, Proteobacteria, Actinobacteria, Firmicutes, Chloroflexi, Acidobacteria, Bacteroidetes and Patescibacteria; Planctomycetes and WPS-2 were the common phyla in NR, BS and VS. Verrucomicrobia was the dominant phylum shared by NR, LR and VS. Myxococcota was the dominant phylum shared by LR, BS and VS. These dominant bacterial phyla accounted for more than 95% of the entire bacterial community (Fig. 6).

In NR, Cyanobacteria, Proteobacteria, Actinobacteria and Firmicutes were the dominant phyla, accounting for more than 80.57% of the relative abundance. The relative abundance of Cyanobacteria in the N1, N3 and N4 treatments was significantly higher than that in the N0 treatment ($p < 0.01$). Compared with cyanobacteria, the relative abundance of Proteobacteria represented an opposite trend. With increasing N addition, the relative abundance of Proteobacteria began to decrease significantly under the N3 treatment and continued to decrease under the N4 treatment ($p < 0.01$). The relative abundance of Firmicutes significantly increased with increasing N addition ($p < 0.01$). In contrast, the relative abundance of Actinobacteria fluctuated with increasing N addition but decreased significantly after N addition in general (Fig. 6 and Table S2). In LR, the relative abundance of four phyla exhibited significant ($p < 0.01$) changes, with a hump-shaped pattern with increasing N addition for

Proteobacteria, Chloroflexi, Acidobacteria and Bacteroidetes, whereas it decreased significantly for Firmicutes ($p < 0.01$) (Fig. 6 and Table S3). In BS, the relative abundance of Acidobacteria decreased with N addition, but that of WPS-2 and Bacteroidetes increased in the N4 and N1 treatments, respectively ($p < 0.05$) (Fig. 6 and Table S4). The relative abundance of Firmicutes and Bacteroidetes displayed significant increasing patterns with N addition in VS but Actinobacteria displayed a decreasing pattern of ($p < 0.05$) (Fig. 6 and Table S5).

LEfSe analysis of species difference

LEfSe (LDA effect size) analysis can be used to compare two or more groups to find species with significant differences (indicator species) between groups. To more accurately describe the functional characteristics of indicator species under different N addition treatments, indicator species at the end of each branch were counted. Cladogram analysis showed that bacterial indicator taxa appeared among different N addition treatments in the four biocolonization types. In NR, *o_Burkholderiales* and *f_Sphingomonadaceae*, *g_Chujaibacter*, *p_Firmicutes* and *c_Bacteroidia*, *g_Alicyclobacillus* and *Ktedonobacteria* were the indicator species of N1, N2, N3 and N4, respectively (Additional file 1: Figure S1). In LR, *g_Rubrobacter*, *f_Nocardioideae*, *f_JG30-KFCM45*, *p_Bacteroidetes*, *g_Bacillus*, *o_Caulobacterales* and *f_Rhizobiaceae*, *f_Xanthobacteraceae*, *o_Burkholderiales* and *g_Rhodanobacter*, *f_Sphingomonadaceae* and *g_Dyella*, *g_Chujaibacter*, *f_Acetobacteraceae* and *o_Chloroplast* were the indicator species of N1, N2, N3 and N4, respectively (Additional file 1: Figure S2). In BS, *c_Gammaproteobacteria* and *f_Ktedonobacteraceae* were the unique indicator species of the N1 and N3

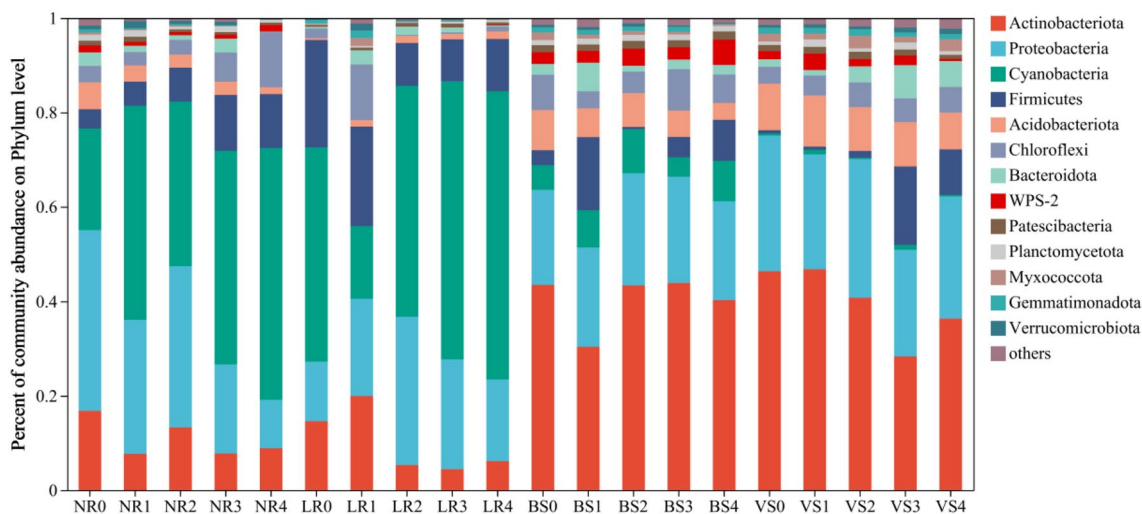


Fig. 6 Community structure composition and relative abundance of bacteria at the phylum level

treatments, respectively, and there were three (o_Rhizobiales, g_Mycobacterium and o_Chloroplast) and four (c_Acidimicrobiia, g_Acidotherrums, g_Conexibater, f_Acetobacteraceae and p_WPS2) indicators of the N2 and N4 treatments, respectively (Additional file 1: Figure S3). There were four (c_Actinobacteria, g_Conexibater, g_Crossiella and p_WPS2), three (c_Acidimicrobiia, f_streptomycetaceae and o_Burkholderiales), four (o_Oscillospirales, g_Lactobacillus, f_Bacteroidaceae and o_Enterobacterales) and two indicator species (o_Gaiellales and o_Rhizobiales) of the N1, N2, N3 and N4 treatments in VS, respectively (Additional file 1: Figure S4). These results indicated that the indicator species appeared differently after N treatment in different biocolonization types.

Linkages of bacterial community composition with environmental factors

Redundancy analysis (RDA) was used to verify the relationships between sample types and environmental factors. The results of RDA showed that all environmental factors explained 86.62%, 81.18%, 71.96% and 63.73% of the variation in bacterial community composition for NR, LR, BS and VS, respectively (Fig. 7A). The environmental factors that contributed the most to the bacterial community composition under different types of biocolonization were TN ($R=0.769$, $p=0.001$, in NR), DON ($R=0.9575$, $p=0.001$, in LR), DON ($R=0.9204$, $p=0.001$, in BS), and TP ($R=0.8178$, $p=0.001$, in VS) (Table S7). Second, environmental factors with significant influence included DON, pH and TOC for NR; TN, pH, DOC and TOC for LR; DOC and pH for BS; and TN, AP, pH and DON for VS (Additional file 1: Table S7). The results demonstrated that the main environmental factors driving bacterial community composition in different types of biocolonization of the Leshan Giant Buddha varied greatly.

Spearman correlation heatmap analysis found that there were twelve bacterial phyla that represented significant correlations with TN in NR (nine were negative and three were positive); all four bacterial phyla displayed positive correlations with DON in LR; two bacterial phyla showed positive correlations and five showed negative correlations with DON in BS; and four bacterial phyla showed significant correlations with TP in VS (Fig. 7B).

Discussion

The rapid population and economic growth in the 21st century has changed the environment and climate, which needs to be taken into account in the sustainable

conservation of stone monuments. Changing environments alter microbial communities and thus the pattern of biodeterioration [36, 37]. Simulations of future climate scenarios can be used to assess and predict changes in biodeterioration patterns [4]. Therefore, we investigated the response of bacterial communities to N deposition under different types of biocolonization of stone in the Leshan Giant Buddha by simulating atmospheric N deposition.

Responses of soil physicochemical properties to N deposition

Biodeterioration is a ubiquitous phenomenon involving the biogeochemical cycling of carbon, nitrogen and phosphorus. Carbon is the pivotal element in constructing the biological framework of ecosystems, while nitrogen and phosphorus serve as primary limiting factors in biological growth and development. They exert a crucial influence on microbial metabolism regulation and dominance, operating independently yet mutually influencing each other [38, 39]. Previous studies have shown that the accumulation of nutrients on the surface of stone relics can promote the growth of epilithic microorganisms, thus increasing the risk of stone degradation [40].

The supersaturation of N causes the pH of the ecosystem to decrease [41]. The addition of ammonium nitrate solution significantly increases the contents of NH_4^+ and NO_3^- in the system. The NO_3^- produced by the nitrification of NH_4^+ and the leaching of excess NO_3^- in the soil are the main mechanisms leading to soil acidification [42]. The H^+ produced by nitrification is adsorbed in the soil cement structure and undergoes a displacement reaction with base ions, resulting in a significant drop in soil pH. The opposite change trend of ammonium nitrogen, nitrate nitrogen and pH value with the increase in N application concentration in NR, LR and BS areas of the Leshan Giant Buddha also confirmed the view that N increase will lead to soil acidification (Fig. 2I). Previous studies have shown that low pH facilitates the precipitation of mineral cations and has a promoting effect on stone degradation [43, 44]. Nitrogen fertilization significantly reduced the soil pH of the four biocolonization types, implying that N deposition had a potential promoting effect on the weathering of the Leshan Giant Buddha under different biocolonization types.

Atmospheric N is an essential nutrient source for ecosystems and can promote primary production under the premise that it does not exceed the critical load of

(See figure on next page.)

Fig. 7 Redundancy analysis between bacterial community and environmental factors (A); heat map analysis of correlations between bacterial phyla and environmental factors (B)

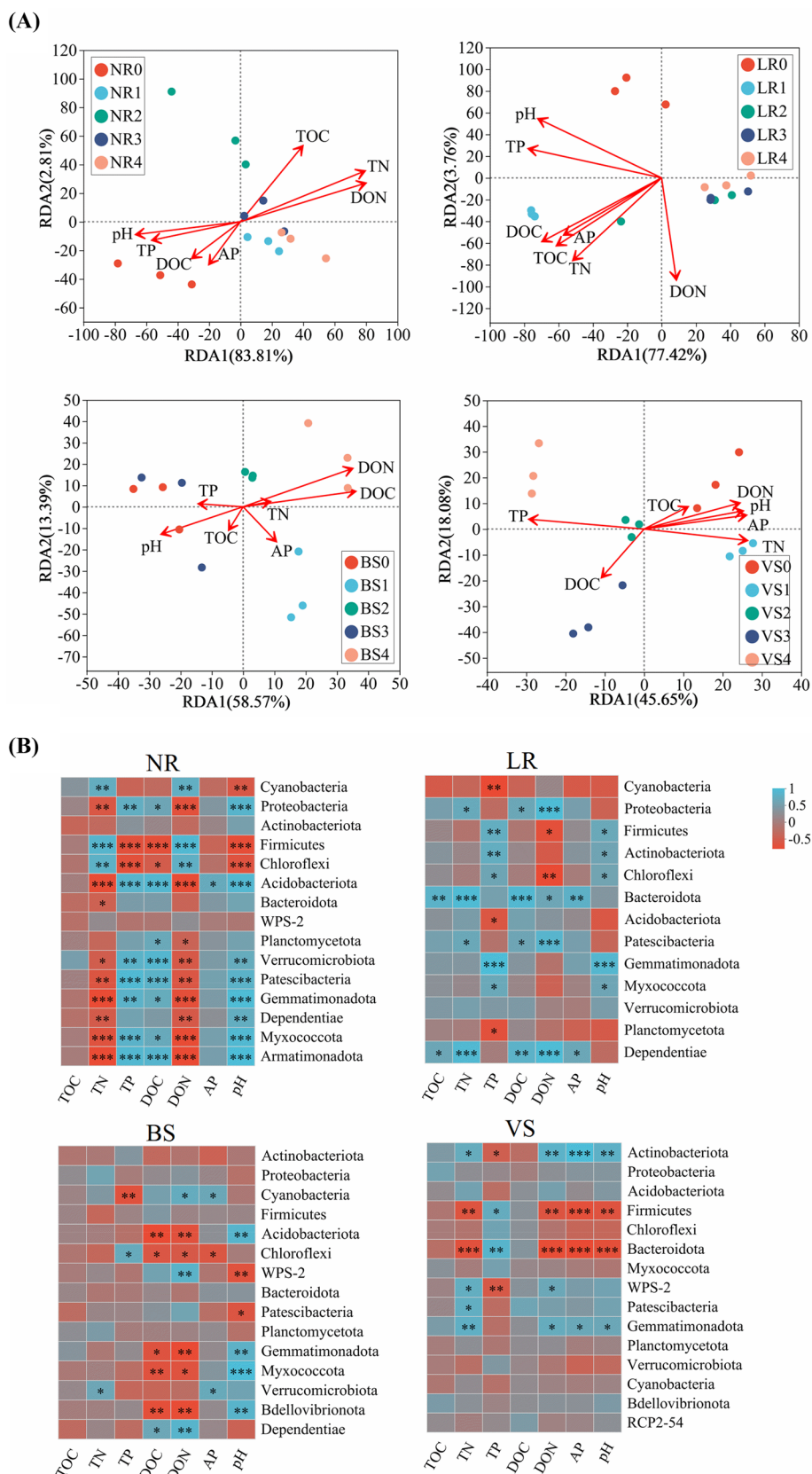


Fig. 7 (See legend on previous page.)

the ecosystem [45]. The results showed that the TOC and TN contents in the NR and LR areas of the Leshan Giant Buddha increased significantly after N addition (Fig. 2A and B). Naked rock and lichen habitats can be regarded as the initial phases of pedogenesis where space replaces time and are typical nitrogen-limited and carbon-deficient ecosystems [46]. Carbon accumulation on stone surfaces mainly consists of microbial biomass. Ortega-Morales et al. (1999) showed that the C/N ratios of biofilm samples collected under different microclimate conditions were close to those of microbial cells, indicating that the main source of organic matter is the biofilm itself [47]. The stimulation of N input promotes carbon assimilation by epilithic microorganisms and increases carbon accumulation on the stone surface by retaining the assimilated carbon in biomass, which is an essential nutrient to support large-scale stone destruction [48]. The positive impact of N deposition on carbon sinks, however, diminished as N saturation increased (Fig. 2A), potentially due to the decline in pH resulting from N addition. Research has indicated that soil acidification can trigger aluminum toxicity in soil microorganisms, consequently leading to a reduction in microbial biomass [49, 50]. In natural ecosystems, the sources of soil organic carbon mainly include the deposition of plant roots and the accumulation of litter [51]. Atmospheric N_r deposition increases the soil available N content to increase crop or tree growth and yield by increasing the plant photosynthetic rate and adjusting carbon allocation [52, 53]. However, N addition did not significantly promote soil TOC accumulation in BS and VS (Fig. 2A), which is similar to the results of many studies on the effect of N addition on organic carbon [54–56]. This is precisely because aboveground vascular plants adjusted their investment strategies in time to directly use the additional inorganic nitrogen, which lessened the necessity for them to cooperate with microorganisms to obtain nutrients and thus did not increase carbon investment into the ground without discrimination [57]. However, organic carbon accumulation is a long-term and slow process in forest ecosystems. Therefore, the 24-month N fertilization treatment in this study was not enough to make the effect of litter input on organic carbon accumulation significant. However, 27 years of N fertilization significantly promoted soil carbon sequestration in grassland ecosystems [58]. This evidence indicated that the accumulation of soil organic carbon by N fertilization depends on the trade-off of benefits by aboveground plant communities and is limited by time, and appropriate N addition may lead to accumulation effects on a larger time scale.

Primary mineral phosphorus is the main form of phosphorus in soil, which becomes the initial source of soil available phosphorus after weathering [59, 60]. The

primary mineral phosphorus is particularly sensitive to soil pH and has low stability in acidic soils [61]. N deposition stimulates proton (H⁺) production and causes soil acidification, which largely drives the dissolution of primary mineral phosphorus [49]. This explained the significant decrease in soil TP content in NR and LR after N addition in this study (Fig. 2C). In addition, the Leshan Giant Buddha is located in a warm and humid subtropical monsoon climate zone, and abundant rainfall is one of the causes of mineralization of primary phosphorus by N, especially when N and rainfall occur simultaneously on the stone surface without vegetation coverage. Zhang et al. (2020) found that the main mineral phosphorus decreased with increasing precipitation [62]. This is because precipitation causes leaching of highly mobile exchangeable calcium ions in the soil [63]. To maintain the charge balance of the soil solution, the calcium-containing primary minerals are dissolved to replenish the soil solution that has lost calcium, and during this process, the associated phosphorus in the primary minerals is also released into the soil solution [64]. Therefore, N deposition can directly lead to the dissolution of primary minerals through soil acidification to release phosphorus. At the same time, precipitation accompanied by N deposition can lead to the leaching of calcium ions and strengthen the weathering of primary minerals [63], resulting in the loss of phosphorus. We also found that the soil TP content in areas of vascular plant colonization increased significantly after N application (Fig. 2C), which may be due to the role of plants and soils buffering the leaching of phosphorus by precipitation accompanied by N deposition and retaining phosphorus in the soil environment through biochemical processes. On one hand, nitrogen deposition can facilitate the release of carboxylates from the plant rhizosphere, thereby accelerating phosphate mineralization of parent rock [65]. On the other hand, immobile particles in the soil and competing sorption sites on otherwise non-polluting sediments and colloids, which are relatively mobile in water flows along the surface or through the soil, exhibit a strong adsorption effect on various forms of phosphorus [66]. The TP content in BS did not show a significant increase as a result of bryophyte rhizoid and barren soil.

Effect of N deposition on the diversity and composition of bacterial communities

Increased nutrient availability has been shown to alter microbial community structure and diversity [67, 68]. The exposed stone surface can be considered a barren ecosystem, limited by many nutrients. Typically, additional available N input increases microbial nutrient availability, promoting microbial community abundance and diversity by alleviating resource constraints

[20]. However, bacterial Shannon diversity decreased significantly with N addition in NR (Fig. 3A), which is consistent with some results on the effect of nitrogen deposition on soil microbial diversity [19, 69]. It is generally accepted that aboveground plants provide carbon to belowground microorganisms through photosynthesis in exchange for other soil nutrients such as N [70]. When soil N availability increases, aboveground plants will maximize their benefits by reducing belowground carbon input, which will lead to a decrease in soil microbial diversity [71]. Clearly, the absence of vegetation in naked stone habitats does not appear to be sufficient evidence that the reduction in bacterial diversity is due to altered carbon allocation strategies of aboveground vegetation. Cyanobacteria are a class of chlorophyll-containing, photosynthetic autotrophic bacteria. Notably, the relative abundance of Cyanobacteria accounted for an average of 40.07% in NR, and it increased significantly (from 21.51 to 45.38%) after N1 application (Table S2). Increased N availability might restrict the carbon release by cyanobacterial autotrophs. This could limit the growth of other bacteria, resulting in reduced bacterial diversity post N-fertilization. In addition, the decrease in bacterial diversity may be related to the decrease in soil pH caused by N input [50]. In particular, soil fungi are adapted to a wider range of soil pH values than bacteria due to their thick and interconnected chitinous cell walls [72]. In this case, the bacterial community tends to select the C-strategist to increase competition with fungi, and this selection enables the competing population to maximize the use of light, water, and nutrients at the site and transfer these resources to organisms to obtain more of other resources (such as exchanging with fungi for minerals mobilized by fungal hyphae from stones). The strategy, however, did not work in areas of vascular plant colonization. In these areas, adding nitrogen significantly increased bacterial biodiversity due to the alleviation of soil nitrogen limitation caused by short-term fertilization [73].

Microbes can respond to nutrient input through changes in community structure. In this study, N addition had significant effects on the bacterial community composition of different types of biocolonization in the Leshan Giant Buddha sandstone (Fig. 4A). N deposition can directly or indirectly affect soil microbial communities by changing various soil properties [74, 75]. The results of RDA showed that after N addition, the environmental factors that had the main impact on the microbial community were different in the four types of biocolonization. For example, TN contributed the most to the change in microbial community structure in naked rock, but TP contributed the most to areas colonized by vascular plants. Previous studies on community succession

sequences have confirmed the limitation of nitrogen in early succession and phosphorus in later succession. This is supported by the significant increase in growth-related parameters of trees in the two younger sites due to nitrogen supply, while no significant effect was observed on plant growth in the oldest site. Additionally, phosphorus additions resulted in an increase in plant tissue phosphorus levels [76]. Therefore, it is reasonable to speculate that N input mediates changes in bacterial community structure by alleviating the nutrient limiting state in different habitats. Altered microbial community structure can affect ecosystem functions, including soil element cycling and nutrient accumulation [77]. The Spearman correlation heatmap showed that in NR, the TN content was significantly positively correlated with the relative abundances of Cyanobacteria, Firmicutes and Chloroflexi. Among them, autotrophic bacteria such as Cyanobacteria and Chloroflexi can fix CO₂ and N₂ in the atmosphere, contributing to the accumulation of organic matter on the stone surface and providing basic nutrients for heterotrophic microorganisms and plant colonization [46].

Soil microbial community structure and composition are highly complex, allowing functional redundancy to occur [78]. Functional redundancy means that the loss of a species may not affect ecosystem function because each metabolic function can be performed by several coexisting, taxonomically distinct species [78]. Although N addition reduced bacterial diversity in bare rock, β -diversity decomposition analysis revealed that species replacement, rather than species abundance, was the main contributor to community variation (Figure 5). Thus, the loss of species in part of the habitat is the result of species nestedness and may not affect their functional diversity. Some studies have found that the degree of weathering of stone cultural relics is related to microbial diversity [79, 80], speculating that high microbial diversity increases the risk of biodeterioration of stone monuments [40]. However, under the background of N deposition, epi-lithic bacteria will adjust their adaptation strategies due to changes in ecological factors, such as reducing diversity and increasing the relative abundance of other groups. Therefore, our study highlighted that the bacterial communities of outdoor stone artefacts responded to external environmental changes through different survival strategies under various biocolonization types (habitats), but such strategies were not strongly associated with biodiversity.

Simultaneously, the LEfSe analysis identified enriched bacterial taxa after N addition in different biocolonization types of stone in the Leshan Giant Buddha. The results showed that Burkholderiales, Sphingomonadaceae, *Chujiabacter*, and Bacteroidetes were indicator

species co-occurring in NR and LR after N addition (Additional file 1: Figure S1 and S2). Many studies have shown that Burkholderiales have high mineral weathering efficiency [81, 82], can effectively dissolve phosphorus from apatite and are important phosphorus-dissolving bacteria [83]; they also have the ability to release silicon, aluminium and iron from biotite rocks [84]. Sphingomonadaceae are aerobic photosynthetic bacteria that play important roles in biocrust ecosystems [85]. *Alicyclobacillus*, which was significantly enriched under N4 treatment in NR (Additional file 1: Figure S1), is an acidophilic bacterium with remarkable bioleaching efficiency for mineral elements such as magnesium, aluminium, potassium, calcium, and phosphorus [86]. In addition, indicator species such as *Basillus*, Rhizobiaceae, *Dyella*, *Rubrobacter*, *Rhodanobacter*, and Acetobacteraceae appeared in areas colonized by lichens after N addition (Figure S2), and most of these species have potential weathering ability. For example, *Basillus* has the same weathering ability as Burkholderia by producing self-emulsifying active acids and surfactants to dissolve mineral elements such as phosphorus, silicon, aluminium, and iron [2, 84]. *Dyella* is often isolated on the surface of weathering stones [87], can release aluminium and iron elements from biotite in a nutrient-poor environment [88], and has high silica and aluminium dissolution activity during the weathering of potassium trite [89]. These results indicate that *Dyella* not only has excellent adaptability on oligotrophic stone surfaces but also plays an important role in promoting biodegradation. Rhizobiales and Acidimicrobiia were indicator species coenriched in BS and VS. In addition, Bacteroidaceae and *Lactobacillus* were indicator species in VS. Acidimicrobiia and Bacteroidaceae are mainly related to cellulose degradation [90], and *Lactobacillus* has a strong ability to metabolize carbohydrates and produce acid and can ferment sugars to produce lactic acid or other acids, which have a direct effect on the biodeterioration of stone. Rhizobiales have functions in biological nitrogen fixation and secretion of cellulase. The enrichment of bacterial taxa varies under different biocolonization, with direct rock-corroding and weathering bacteria dominating in NR and LR, while nutrient-transforming bacteria are prevalent in BS and VS. The diverse enrichment outcomes resulting from the N addition all present a potential risk to stone monuments preservation.

The results of our study revealed that the N addition significantly enhanced the accumulation of TOC in both NR and LR. Additionally, it was observed that atmospheric N deposition had a stimulating effect on the enrichment of TP content in VS. These indicate that future increases in N deposition will promote nutrient accumulation in the rock surface of Leshan Giant

Buddha. In NR, the addition of N resulted in a decrease in bacterial diversity; however, the analysis of β -diversity decomposition revealed that community change was primarily driven by species turnover rather than species richness. Meanwhile, the LEfSe analysis found that Burkholderiales and *Alicyclobacillus* bacterial groups were significantly enriched in NR, which had high mineral weathering efficiency on rocks. Previous studies have established a significant correlation between bacterial diversity and the weathering of cultural relics [79, 80]. However, this study emphasizes that species replacement of bacteria plays a greater role in altering community structure within the context of N deposition. Therefore, in order to effectively preserve stone monuments against biodeterioration in areas with increasing nitrogen deposition pollution, it is crucial to focus on specific species and functional bacteria while developing targeted protective measures.

In addition, the mechanism of enriched bacterial groups with potential weathering risk in the weathering process of stone monument requires further investigation. Clarifying the physiological and biochemical key processes of these microorganisms is crucial for formulating specific measures to safeguard and conserve stone monuments in the face of increasing nitrogen deposition in the future.

Conclusions

The impact environmental pollution on the biodeterioration of outdoor immovable stone monuments has received much attention. We investigated the responses of bacterial communities and soil nutrients in four typical biocolonization types of stone in the Leshan Giant Buddha, a world cultural and natural heritage site, by simulating atmospheric nitrogen deposition. We found that nitrogen fertilization promoted the accumulation of total organic carbon and total nitrogen in NR and LR, and increased the content of total phosphorus in VS. Bacterial α -diversity decreased with nitrogen addition in NR but increased with nitrogen addition in VS. Nitrogen addition significantly changed the bacterial community composition in the four biocolonization types, and the changes were dominated by species replacement. The study demonstrates that the future increase in atmospheric nitrogen deposition will enhance nutrient accumulation within the surface layer of stone monuments, consequently augmenting the susceptibility of stone monuments to weathering through alterations in bacterial community structure and composition. The accuracy of cultural relic protection and preservation in the context of climate change can be enhanced by giving more attention to the specific taxa and functional species associated with outdoor stone monuments.

Supplementary Information

The online version contains supplementary material available at <https://doi.org/10.1186/s40494-024-01142-3>.

Additional file 1: Table S1. Permutational multivariate analysis of variance (PERMANOVA) of four biocolonization types. **Table S2.** Relative abundance of bacterial species on phylum level of NR biocolonization under different nitrogen addition treatments (means \pm SD). **Table S3.** Relative abundance of bacterial species on phylum level of LR biocolonization under different nitrogen addition treatments (means \pm SD). **Table S4.** Relative abundance of bacterial species on phylum level of BS biocolonization under different nitrogen addition treatments (means \pm SD). **Table S5.** Relative abundance of bacterial species on phylum level of VS biocolonization under different nitrogen addition treatments (means \pm SD). **Table S6.** Physical and mechanical properties of bare rock and rock under different biocolonization (means \pm SD). **Table S7.** Multivariate direct gradient analysis based on linear models of four biocolonization types. **Figure S1.** LEfSe analysis of bacterial species at various classification levels under different nitrogen addition in NR biocolonization. The branch diagram shows the statistical difference between N0–N4 treatments at LDA level $>$ 4. Circles from different taxonomic represent taxa at that level. The circle from inside to outside represents the rank of classification from phylum to genus. Different nitrogen levels correspond to different colors, representing the microbial groups that play an important role in each group. The name of the taxon is shown on the right of the corresponding picture. The same below. **Figure S2.** LEfSe analysis of bacterial species at various classification levels under different nitrogen addition in LR biocolonization. **Figure S3.** LEfSe analysis of bacterial species at various classification levels under different nitrogen addition in BS biocolonization. **Figure S4.** LEfSe analysis of bacterial species at various classification levels under different nitrogen addition in VS biocolonization.

Acknowledgements

Not applicable.

Author contributions

X.C. was primarily responsible for conducting the investigation and analysis, which included experimental design, data analysis, diagram creation, and manuscript writing. H.S. was assigned with the task of reviewing and revising the manuscript. B.S. was in charge of maintaining and sampling the experimental plot, while T.Y. assumed responsibility for selecting and maintaining the experimental plots. All authors reviewed the manuscript.

Funding

Supported by the Talent Introduction Project Fund of Xihua University (RX2300000787).

Availability of data and materials

The datasets of gene sequences analysed during the current study are available in Genbank with accession SRP451507.

Declarations

Competing interests

The authors declare that they have no competing interests.

Author details

¹College of Fine Arts and Design, Xihua University, Chengdu 610039, China. ²College of Landscape Architecture, Sichuan Agricultural University, Chengdu 611130, China. ³Key Laboratory of Disaster Prevention and Mitigation in Civil Engineering of Lanzhou University of Technology, Lanzhou 730050, Gansu, China. ⁴Leshan Giant Buddha Grottoes Research Institute, Leshan 614003, China.

Received: 12 September 2023 Accepted: 10 January 2024

Published online: 22 January 2024

References

- Negi A, Sarethy IP. Microbial biodeterioration of cultural heritage: events, colonization, and analyses. *Microb Ecol.* 2019;78:1014–29.
- Scheerer S, Ortega-Morales O, Gaylarde C. Microbial deterioration of stone monuments—an updated overview. *Adv Appl Microbiol.* 2009;66:97.
- Bohu T, Anand R, Noble R, Lintern M, Kaksonen AH, Mei Y, Cheng KY, Deng X, Veder J, Bunce M, et al. Evidence for fungi and gold redox interaction under Earth surface conditions. *Nat Commun.* 2019;10:2290.
- Liu X, Koestler RJ, Warscheid T, Katayama Y, Gu J. Microbial deterioration and sustainable conservation of stone monuments and buildings. *Nat Sustain.* 2020;3:991–1004.
- Palmqvist K, Campbell D, Ekblad A, Johansson H. Photosynthetic capacity in relation to nitrogen content and its partitioning in lichens with different photobionts. *Plant Cell Environ.* 1998;21:361–72.
- Hinsinger P, Barros ONF, Benedeth MF, Noack Y, Callot G. Plant-induced weathering of a basaltic rock: experimental evidence. *Geochim Cosmochim Acta.* 2001. [https://doi.org/10.1016/S0016-7037\(00\)00524-X](https://doi.org/10.1016/S0016-7037(00)00524-X).
- Wu F, Zhang Y, He D, Gu J, Guo Q, Liu X, Duan Y, Zhao J, Wang W, Feng H. Community structures of bacteria and archaea associated with the biodeterioration of sandstone sculptures at the Beishiku Temple. *Int Biodeter Biodegr.* 2021;164: 105290.
- Strauss SL, Garcia-Pichel F, Day TA. Soil microbial carbon and nitrogen transformations at a glacial foreland on Anvers Island, Antarctic Peninsula. *Polar Biol.* 2012;35:1459–71.
- Napierski SA, Buss HL, Brantley SL, Lee S, Xu H, Roden EE. Microbial chemolithotrophy mediates oxidative weathering of granitic bedrock. *Proc Natl Acad Sci USA.* 2019;116:26394–401.
- He J, Zhang N, Muhammad A, Shen X, Sun C, Li Q, Hu Y, Shao Y. From surviving to thriving, the assembly processes of microbial communities in stone biodeterioration: a case study of the West Lake UNESCO World Heritage area in China. *Sci Total Environ.* 2022;805: 150395.
- Li Q, Zhang B, He Z, Yang X. Distribution and diversity of bacteria and fungi colonization in stone monuments analyzed by high-throughput sequencing. *PLoS ONE.* 2016;11:e163287.
- Liu Y, Tan X, Wang Y, Guo Z, He D, Fu S, Wan S, Ye Q, Zhang W, Liu W, et al. Responses of litter, organic and mineral soil enzyme kinetics to 6 years of canopy and understory nitrogen additions in a temperate forest. *Sci Total Environ.* 2020;712: 136383.
- Fowler D, Pyle JA, Raven JA, Sutton MA. The global nitrogen cycle in the twenty-first century: introduction. *Philos Trans R Soc B Biol Sci.* 2013;368:20130165.
- Galloway JN, Townsend AR, Erisman JW, Bekunda M, Cai Z, Freney JR, Martinelli LA, Seitzinger SP, Sutton MA. Transformation of the nitrogen cycle: recent trends, questions, and potential solutions. *Science.* 2008;320:889–92.
- Galloway JN, Dentener FJ, Capone DG, Boyer EW, Howarth RW, Seitzinger SP, Asner GP, Cleveland CC, Green PA, Holland EA, et al. Nitrogen cycles: past, present, and future. *Biogeochemistry.* 2004;70:153–226.
- Liu X, Zhang Y, Han W, Tang A, Shen J, Cui Z, Vitousek P, Erisman JW, Goulding K, Christie P, et al. Enhanced nitrogen deposition over China. *Nature.* 2013;494:459–62.
- Sheng W, Yu G, Jiang C, Yan J, Liu Y, Wang S, Wang B, Zhang J, Wang C, Zhou M, et al. Monitoring nitrogen deposition in typical forest ecosystems along a large transect in China. *Environ Monit Assess.* 2013;185:833–44.
- Zhu J, He N, Wang Q, Yuan G, Wen D, Yu G, Jia Y. The composition, spatial patterns, and influencing factors of atmospheric wet nitrogen deposition in Chinese terrestrial ecosystems. *Sci Total Environ.* 2015;511:777–85.
- Wang J, Shi X, Zheng C, Suter H, Huang Z. Different responses of soil bacterial and fungal communities to nitrogen deposition in a subtropical forest. *Sci Total Environ.* 2021;755: 142449.
- Knelman JE, Schmidt SK, Lynch RC, Darcy JL, Castle SC, Cleveland CC, Nemergut DR. Nutrient addition dramatically accelerates microbial community succession. *PLoS ONE.* 2014;9: e102609.
- Treseder KK. Nitrogen additions and microbial biomass: a meta-analysis of ecosystem studies. *Ecol Lett.* 2008;11:1111–20.
- Qiao Z, Ding Z, Wang J, Sun B, Wang F, Xie Z. Enhanced mechanical properties and environmental erosion resistance with metakaolin in a kind of Chinese traditional Lime-based mortar. *Constr Build Mater.* 2022;317: 126110.

23. Chen X, Wang M, Wu F, Sun B, Yang T, Song H. Soil bacteria and fungi respond differently to organisms covering on Leshan Giant Buddha Body. *Sustainability*. 2021;13: 3897.
24. Leysen L, Roekens E, Van Grieken R. Air-pollution-induced chemical decay of a sandy-limestone cathedral in Belgium. *Sci Total Environ*. 1989;78:263–87.
25. Kaijun Y, Wanqin Y, Liyan Z, Zhi-jie L, Ruo-yang H, Bo T, Li Z, Jiu-jin X, Zhen-Feng X. Characteristics of atmospheric wet nitrogen deposition in Dujiangyan, western edge of Sichuan basin. *Chin J Appl Environ Biol*. 2018;01:107–11.
26. Zhou Y, Sun B, Xie B, Feng K, Zhang Z, Zhang Z, Li S, Du X, Zhang Q, Gu S, et al. Warming reshaped the microbial hierarchical interactions. *Glob Change Biol*. 2021;27:6331–47.
27. Ji-dong Z, Rong-jiu S, Feng Z, Si-qin H, Ying Z. Effects of the frequency and intensity of nitrogen addition on soil pH, the contents of carbon, nitrogen and phosphorus in temperate steppe in Inner Mongolia China. *Ying Yong Sheng TaiXue Bao*. 2016;8:2467–76.
28. Liu J, Shu A, Song W, Shi W, Li M, Zhang W, Li Z, Liu G, Yuan F, Zhang S, et al. Long-term organic fertilizer substitution increases rice yield by improving soil properties and regulating soil bacteria. *Geoderma*. 2021;404: 115287.
29. Apprill A, McNally S, Parsons R, Weber L. Minor revision to V4 region SSU rRNA 806R gene primer greatly increases detection of SAR11 bacterioplankton. *Aquat Microb Ecol*. 2015;75:129–37.
30. Mori H, Maruyama F, Kato H, Toyoda A, Dozono A, Ohtsubo Y, Nagata Y, Fujiyama A, Tsuda M, Kurokawa K. Design and experimental application of a novel non-degenerate universal primer set that amplifies prokaryotic 16S rRNA genes with a low possibility to amplify eukaryotic rRNA genes. *DNA Res*. 2014;21:217–27.
31. Edgar RC. UPARSE: highly accurate OTU sequences from microbial amplicon reads. *Nat Methods*. 2013;10:996–8.
32. Stackebrandt E, Goebel BM. Taxonomic note: a place for DNA-DNA reassociation and 16S rRNA sequence analysis in the present species definition in bacteriology. *Int J Syst Evol Microbiol*. 1994;44:846–9.
33. Wang Q, Garrity GM, Tiedje JM, Cole JR. Naive bayesian classifier for rapid assignment of rRNA sequences into the new bacterial taxonomy. *Appl Environ Microb*. 2007;73:5261–7.
34. Shen C, Gunina A, Luo Y, Wang J, He JZ, Kuzyakov Y, Hemp A, Classen AT, Ge Y. Contrasting patterns and drivers of soil bacterial and fungal diversity across a mountain gradient. *Environ Microbiol*. 2020;22:3287–301.
35. Li W, Sheng H, Ekawati D, Jiang Y, Yang H. Variations in the compositions of soil bacterial and fungal communities due to microhabitat effects induced by simulated nitrogen deposition of a bamboo forest in wetland. *Forests*. 2019;10: 1098.
36. Caneva G, Bartoli F, Savo V, Futagami Y, Strona G. Combining statistical tools and ecological assessments in the study of biodeterioration patterns of stone temples in Angkor (Cambodia). *Sci Rep*. 2016;6: 632601.
37. Caneva G, Bartoli F, Ceschin S, Salvadori O, Futagami Y, Salvati L. Exploring ecological relationships in the biodeterioration patterns of Angkor temples (Cambodia) along a forest canopy gradient. *J Cult Herit*. 2015;16:728–35.
38. Fan Y, Lin F, Yang L, Zhong X, Wang M, Zhou J, Chen Y, Yang Y. Decreased soil organic P fraction associated with ectomycorrhizal fungal activity to meet increased P demand under N application in a subtropical forest ecosystem. *Biol Fertil Soils*. 2018;54:149–61.
39. You C, Wu F, Yang W, Xu Z, Tan B, Zhang L, Yue K, Ni X, Li H, Chang C, et al. Does foliar nutrient resorption regulate the coupled relationship between nitrogen and phosphorus in plant leaves in response to nitrogen deposition? *Sci Total Environ*. 2018;645:733–42.
40. Mitchell R, Gu J. Changes in the biofilm microflora of limestone caused by atmospheric pollutants. *Int Biodeter Biodegrad*. 2000;46:299–303.
41. Rousk J, Bååth E, Brookes PC, Lauber CL, Lozupone C, Caporaso JG, Knight R, Fierer N. Soil bacterial and fungal communities across a pH gradient in an arable soil. *ISME J*. 2010;4:1340–51.
42. Fierer N, Jackson RB. The diversity and biogeography of soil bacterial communities. *Proc Natl Acad Sci*. 2006;103:626–31.
43. Samuels T, Pybus D, Wilkinson M, Cockell CS. pH influences the distribution of microbial rock-weathering phenotypes in weathered shale environments. *Geomicrobiol J*. 2019;36:752–63.
44. Ali AM, Padmanabhan E, Mijinyawa A, Kwaya MY. Effect of pH on the stability of quartz in a multi-phase system of kaolinite, hydrous Al (hydr) oxide and quartz. *Sn Appl Sci*. 2019;1:1.
45. Sun M, Li M, Zhou Y, Liu J, Shi W, Wu X, Xie B, Deng Y, Gao Z. Nitrogen deposition enhances the deterministic process of the prokaryotic community and increases the complexity of the microbial co-network in coastal wetlands. *Sci Total Environ*. 2023;856: 158939.
46. Liu Y, Lu M, Zhang X, Sun Q, Liu R, Lian B. Shift of the microbial communities from exposed sandstone rocks to forest soils during pedogenesis. *Int Biodeter Biodegrad*. 2019;140:21–8.
47. Ortega-Morales BO, Herna Ndez-Duque G, Borges-Go Mez L, Guezenec J. Characterization of epilithic microbial communities associated with mayan stone monuments in Yucatan. *Mexico Geomicrobiol*. 1999;16:221–32.
48. Salvadori O, Municchia AC. The role of fungi and lichens in the biodeterioration of stone monuments. *Open Conf Proc J*. 2016;7:39–54.
49. Tian D, Niu S. A global analysis of soil acidification caused by nitrogen addition. *Environ Res Lett*. 2015;10: 24019.
50. Tian D, Jiang L, Ma S, Fang W, Schmid B, Xu L, Zhu J, Li P, Losapio G, Jing X, et al. Effects of nitrogen deposition on soil microbial communities in temperate and subtropical forests in China. *Sci Total Environ*. 2017;607–608:1367–75.
51. Ma W, Wu F, Tian T, He D, Zhang Q, Gu J, Duan Y, Ma D, Wang W, Feng H. Fungal diversity and its contribution to the biodeterioration of mural paintings in two 1700-year-old tombs of China. *Int Biodeter Biodegrad*. 2020;152: 104972.
52. Zhang C, Liu G, Xue S, Wang G. Soil bacterial community dynamics reflect changes in plant community and soil properties during the secondary succession of abandoned farmland in the Loess Plateau. *Soil Biol Biochem*. 2016;97:40–9.
53. Vitousek P, Howarth R. Nitrogen limitation on land and in the sea: how can it occur? *Biogeochemistry*. 1991;13:87–115.
54. Silveira ML, Liu K, Sollenberger LE, Follett RF, Vendramini JMB. Short-term effects of grazing intensity and nitrogen fertilization on soil organic carbon pools under perennial grass pastures in the southeastern USA. *Soil Biol Biochem*. 2013;58:42–9.
55. Janssens IA, Dieleman W, Luyssaert S, Subke J, Reichstein M, Ceulemans R, Ciais P, Dolman AJ, Grace J, Matteucci G, et al. Reduction of forest soil respiration in response to nitrogen deposition. *Nat Geosci*. 2010;3:315–22.
56. Nave LE, Vance ED, Swanston CW, Curtis PS. Impacts of elevated N inputs on north temperate forest soil C storage, C/N, and net N-mineralization. *Geoderma*. 2009;153:231–40.
57. Haynes BE, Gower ST. Belowground carbon allocation in unfertilized and fertilized red pine plantations in northern Wisconsin. *Tree Physiol*. 1995;15:317–25.
58. Fornara DA, Tilman D. Soil carbon sequestration in prairie grasslands increased by chronic nitrogen addition. *Ecology*. 2012;93:2030–6.
59. Helfenstein J, Tamburini F, von Sperber C, Massey MS, Pistocchi C, Chadwick OA, Vitousek PM, Kretzschmar R, Frossard E. Combining spectroscopic and isotopic techniques gives a dynamic view of phosphorus cycling in soil. *Nat Commun*. 2018;9:3226.
60. Yang X, Post WM. Phosphorus transformations as a function of pedogenesis: a synthesis of soil phosphorus data using Hedley fractionation method. *Biogeosciences*. 2011;8:2907–16.
61. Helfenstein J, Pistocchi C, Oberson A, Tamburini F, Goll DS, Frossard E. Estimates of mean residence times of phosphorus in commonly considered inorganic soil phosphorus pools. *Biogeosciences*. 2020;17:441–54.
62. Zhang H, Shi L, Fu S. Effects of nitrogen deposition and increased precipitation on soil phosphorus dynamics in a temperate forest. *Geoderma*. 2020;380: 114650.
63. Austin AT, Yahdjian L, Stark JM, Belnap J, Porporato A, Norton U, Ravetta DA, Schaeffer SM. Water pulses and biogeochemical cycles in arid and semiarid ecosystems. *Oecologia*. 2004;141:221–35.
64. Lerman A, Wu L. Kinetics of global geochemical cycles. New York: Springer; 2008. p. 655–736.
65. Ding W, Cong W, Lambers H. Plant phosphorus-acquisition and -use strategies affect soil carbon cycling. *Trends Ecol Evol*. 2021;36:899–906.
66. McGeachan MB, Lewis DR. SW—soil and water. *Biosyst Eng*. 2002;82:1–24.
67. Widdig M, Heintz-Buschart A, Schleuss P, Guhr A, Borer ET, Seabloom EW, Spohn M. Effects of nitrogen and phosphorus addition on microbial

- community composition and element cycling in a grassland soil. *Soil Biol Biochem.* 2020;151: 108041.
68. Leff JW, Jones SE, Prober SM, Barberán A, Borer ET, Firn JL, Harpole WS, Hobbie SE, Hofmockel KS, Knops JMH, et al. Consistent responses of soil microbial communities to elevated nutrient inputs in grasslands across the globe. *Proc Natl Acad Sci.* 2015;112:10967–72.
 69. Wang C, Lu X, Mori T, Mao Q, Zhou K, Zhou G, Nie Y, Mo J. Responses of soil microbial community to continuous experimental nitrogen additions for 13 years in a nitrogen-rich tropical forest. *Soil Biol Biochem.* 2018;121:103–12.
 70. Vasar M, Andreson R, Davison J, Jairus T, Moora M, Remm M, Young JPW, Zobel M, Öpik M. Increased sequencing depth does not increase captured diversity of arbuscular mycorrhizal fungi. *Mycorrhiza.* 2017;27:761–73.
 71. Johnson IT, Thornley JH. A model of shoot: Root partitioning with optimal growth. *Ann Bot.* 1987;60:133–42.
 72. Nielsen UN, Ball BA. Impacts of altered precipitation regimes on soil communities and biogeochemistry in arid and semi-arid ecosystems. *Glob Change Biol.* 2015;21:1407–21.
 73. Guo P, Jia J, Han T, Xie J, Wu P, Du Y, Qu K. Nonlinear responses of forest soil microbial communities and activities after short- and long-term gradient nitrogen additions. *Appl Soil Ecol.* 2017;121:60–4.
 74. Shi X, Hu H, Wang J, He J, Zheng C, Wan X, Huang Z. Niche separation of comammox Nitrospira and canonical ammonia oxidizers in an acidic subtropical forest soil under long-term nitrogen deposition. *Soil Biol Biochem.* 2018;126:114–22.
 75. Romanowicz KJ, Freedman ZB, Upchurch RA, Argiroff WA, Zak DR, Univ O, Michigan AAMU, Baldrian P. Active microorganisms in forest soils differ from the total community yet are shaped by the same environmental factors: the influence of pH and soil moisture. *Fems Microbiol Ecol.* 2016;10:10.
 76. Vitousek PM, Walker LR, Whiteaker LD, Matson PA. Nutrient limitations to plant growth during primary succession in Hawaii Volcanoes National Park. *Biogeochemistry.* 1993;23:197–215.
 77. Delgado Baquerizo M, Giaramida L, Reich PB, Khachane AN, Hamonts K, Edwards C, Lawton LA, Singh BK. Lack of functional redundancy in the relationship between microbial diversity and ecosystem functioning. *J Ecol.* 2016;104:936–46.
 78. Louca S, Polz MF, Mazel F, Albright MBN, Huber JA, O Connor MI, Ackermann M, Hahn AS, Srivastava DS, Crowe SA, et al. Function and functional redundancy in microbial systems. *Nat Ecol Evol.* 2018;2:936–43.
 79. Ma GY, He LY, Sheng XF. Characterization of bacterial community inhabiting the surfaces of weathered bricks of Nanjing Ming City walls. *Sci Total Environ.* 2011;409(4):756–62.
 80. Santelli CM, Edgcomb VP, Bach W, Edwards KJ. The diversity and abundance of bacteria inhabiting seafloor lavas positively correlate with rock alteration. *Environ Microbiol.* 2009;11:86–98.
 81. Leveau JH, Uroz S, de Boer W. The bacterial genus *Collimonas*: mycophagy, weathering and other adaptive solutions to life in oligotrophic soil environments. *Environ Microbiol.* 2010;12:281–92.
 82. Uroz S, Calvaruso C, Turpault M, Frey-Klett P. Mineral weathering by bacteria: ecology, actors and mechanisms. *Trends Microbiol.* 2009;17:378–87.
 83. Pastore G, Kernchen S, Spohn M. Microbial solubilization of silicon and phosphorus from bedrock in relation to abundance of phosphorus-solubilizing bacteria in temperate forest soils. *Soil Biol Biochem.* 2020;151: 108050.
 84. Yu Y, Sheng X, He L, Huang Z. Linkage between culturable mineral-weathering bacteria and their weathering effectiveness along a soil profile. *Geomicrobiol J.* 2016;33:10–9.
 85. Tang K, Yuan B, Jia L, Pan X, Feng F, Jin K. Spatial and temporal distribution of aerobic anoxygenic phototrophic bacteria: key functional groups in biological soil crusts. *Environ Microbiol.* 2021;23:3554–67.
 86. Issayeva A, Pankiewicz R, Otarbekova A. Bioleaching of metals from wastes of phosphoric fertilizers production. *Pol J Environ Stud.* 2020;29:4101–8.
 87. Zhao F, Guo X, Wang P, He L, Huang Z, Sheng X. *Dyella jiangningensis* sp. nov., a γ -proteobacterium isolated from the surface of potassium-bearing rock. *Int J Syst Evol Microbiol.* 2013;63:3154–7.
 88. Bao Y, Kwok AHY, He L, Jiang J, Huang Z, Leung FC, Sheng X. Complete genome sequence of *Dyella jiangningensis* strain SBZ3-12, isolated from the surfaces of weathered rock. *Genome Announc.* 2014;2:e00416-14-e00416-14.
 89. Wang Y, Zhang H, Liu X, Liu X, Song W. Fungal communities in the biofilms colonizing the basalt sculptures of the Leizhou Stone Dogs and assessment of a conservation measure. *Herit Sci.* 2021;9:9.
 90. Pop Ristova P, Bienhold C, Wenzhöfer F, Rossel PE, Boetius A. Temporal and spatial variations of bacterial and faunal communities associated with deep-sea wood falls. *PLoS ONE.* 2017;12: e169906.

Publisher's Note

Springer Nature remains neutral with regard to jurisdictional claims in published maps and institutional affiliations.